Ruthenium-Based Electrode Modified by Gold Particles as Voltammetric Sensor for Non-Enzymatic Epinephrine Detection

Maxim S. Panov[1,2,3], Dmitrii M. Nikolaev[3,4], Andrey A. Shtyrov[3,4], Sergey Yu. Vyazmin[3], Andrey S. Mereshchenko[1], Andrey V. Vasin[4,5], Mikhail N. Ryazantsev[1,3*]

1 Institute of Chemistry, Saint Petersburg State University, 26 Universitetskii pr, St. Petersburg, 198504, Russian Federation
2 St. Petersburg State Chemical Pharmaceutical University, Professor Popov str., 14, lit. A, St. Petersburg, 197022, Russian Federation
3 Saint Petersburg Academic University, 8/3 Khlopina Street, St. Petersburg, 194021, Russian Federation
4 Institute of Biomedical Systems and Biotechnologies, Peter the Great St. Petersburg Polytechnic University, 29 Polytechnicheskaya Str., St. Petersburg, 195251, Russian Federation
5 Smorodintsev Research Institute of Influenza, 15/17, Prof. Popov Str., 197376 St. Petersburg, Russian Federation

* mikhail.n.ryazantsev@gmail.com

Abstract

A simple and efficient technique for voltammetric enzymeless detection of epinephrine (EP) is proposed. The technique applies hierarchical Ru-based electrodes modified by Au nano- to micro-sized particles, which were produced with laser-assisted synthesis. The cyclic voltammetry (CV) and differential pulse voltammetry (DPV) were employed to characterize electrochemical properties of the electrodes. For EP detection, we obtained two DPV calibration curves that are linear in the range of 0.01-5 μM and 5-500 μM. The highest sensitivity (46.9 μA μM^{-1} cm^{-2}) and the lowest detection limit (6.1 nM) are observed for the first linear range, whereas the estimated sensitivity and limit of detection for the second linear range are 2.1 μA μM^{-1} cm^{-2} and 17.8 nM, respectively. We also demonstrated that the proposed technique can be used for selective EP determination in the presence of such common interfering analytes as ascorbic acid and dopamine. The results of this study can be employed for development of low-cost voltammetric sensor platforms for non-enzymatic epinephrine detection in a physiological environment.

Introduction

Epinephrine (EP or adrenaline) is both a hormone and a neurotransmitter. This compound interacts with receptors of internal organs and blood vessels regulating their functions and participates in the transmission of nerve impulses of the sympathetic nervous system [1]. EP is formed in the adrenal glands and can be considered as one of the hormones that is responsible for the body's response to stress. EP is involved in many physiological processes, such as increasing heart rate, regulation of blood pressure, enhancement of lipolysis, bronchial dilation, control of the blood sugar level, etc [2]. EP is also a medication that is intensively used in emergency healthcare [3, 4].

Monitoring and maintaining the EP concentration within the physiological range, which is between a few and tens of nM, is of special importance and any imbalance in the concentration of this compound can lead to several serious diseases such as Parkinson's disease [5], schizophrenia [6] and Alzheimer's disease [7]. There are several reasons why detection of biomarkers such as epinephrine is difficult. First, epinephrine, as other representatives of the catecholamines group to which it belongs, is hydrophobic and its concentration in biological fluids, such as blood or urine, is very low [1]. Second, these species are short-lived in the blood [8]. Third, EP is easily oxidized to a highly reactive intermediate, adrenalinchrome, which can form polymers capable of blocking the surface of an electrode [8]. Finally, it is very hard to perform selective electrochemical analysis of EP in the presence of other important bioanalytes such as ascorbic acid and dopamine because of the proximity of their oxidation potentials.

Several methods have been proposed for detection of epinephrine (see [8] for review). The voltammetric methods have a number of advantages among others. Thus, the electrochemical approach is very simple, cheap and highly sensitive; moreover, it does not require a long analysis time [1, 9]. In turn, voltammetric sensors applied to detect biomolecules can be divided into two types [10, 11]. The first type includes sensors, in which enzymes are used as specific elements for the analyte recognition [10]. Despite the good sensitivity and selectivity demonstrated by the enzymatic sensors, they are expensive and difficult to prepare, suffer from low stability and reproducibility, and also they are rather sensitive to temperature and pH. In contrast, the sensors of the second type do not contain enzymes, but employ materials with high electrocatalytic activity; the enzyme-free oxidation of an analyte proceeds directly on the electrode surface [12,13].

The most appropriate materials for enzyme-free sensing of hydrophobic metabolites, including epinephrine, are based on metal-containing structures [14–20]. In this regard, micro- and nanoscale bimetallic structures obtained in various forms such as bimetallic particles, heterophase eutectic alloys and composite materials with pronounced interphase interaction can be considered the most promising [21–26]. Many techniques can be employed to fabricate such bimetallic structures, including direct laser writing [27], chemical vapor deposition [28], inkjet printing [29], laser ablation [30], laser sintering [31] and others [32, 33]. The laser-induced chemical liquid phase deposition of metals (LCLD) [34] used in this study is a representative of the laser-based techniques with the strength and weakness inherent to these techniques [33, 35–38]. The strong sides of LCLD approach are: 1) the capability to metallize the dielectric surfaces with a large band gap such as glass or glass-ceramics without additional preparation; 2) the capability to localize the reaction in a small (several tens of microns) volume within the size of the focused laser beam; 3) the capability to deposit conductive metallic and bimetallic materials with a highly developed surface areas, which is especially important to detect a low concentration of analytes; 4) within the LCLD framework, it is possible to carry out the synthesis of micro- and nanostructures from dissolved metal salt continuously, i.e. directly in the reaction mixture and practically without changing its composition during the process. Structures with highly developed surfaces and excellent electrochemical properties that are based on Cu [39], Au [24], Pt [40], Ir [41], Ru [42] and other metals were already obtained using this method.

In this study, we applied the LCLD technique to develop a voltammetric sensor based on Ru structures modified by Au nanoparticles (AuNPs) to be used for the enzyme-free determination of EP. The choice of Ru and Au was related to their outstanding electrical and catalytic properties. The highly developed electroactive surface of the Ru-based electrodes fabricated by the LCLD technique was enhanced by Au nanoparticles to provide additional active centers. The performance of the obtained sensor has been evaluated both in the pure phosphate-buffered saline solution and in the presence of such common interfering agents as ascorbic acid and dopamine.

Materials and Methods

Laser-induced synthesis of Ru and its modification by Au particles

All chemicals used in the current study were purchased from Sigma Aldrich (St. Louis, USA). The layout of the experimental setup can be found elsewhere [24, 34, 43]. Briefly, the 532-nm output from a diode-pumped continuous-wave solid-state Nd:YAG laser (Changchun, China) was focused at the interface between the glass window used as the substrate and the plating solution in the experimental cell. The diameter of the focused by a microscope objective (15-mm focus length) laser beam was 10 μm. The cell could be translated in three dimensions by a computer-controlled XYZ motorized platform to "draw" metallic structures of different shape and size. The small portion of the output light was reflected from the front glass window of the cell and redirected toward a web-camera for monitoring the metal deposition process.

The laser-assisted fabrication of Ru-Au composite was performed in two steps. First, we carried out laser-assisted deposition of Ru from DMF (N, N-dimethylformamide) solution of 5 mM $Ru_3(CO)_{12}$ (triruthenium dodecacarbonyl) on the surface of glass at the laser power density of $\sim$2.3mW/μm^2 and at the scanning speed of 5 μm/s. The resulting Ru-based structures (electrodes) were 10 mm in length and $\sim$145 μm in width. Second, we performed laser-assisted deposition of Au particles from colloidal solution containing Au nanoparticles (see below) on the surface of the fabricated Ru structures at the same scanning speed and at the laser power density of 2.5 $\sim$mW/μm^2.

The preparation method of the colloidal solution with Au nanoparticles is described in [44]. The 95 mL of distilled water was poured into a clean conical flask, then 30 mL of a 30% solution of $HAuCl_4$ (hydrogen tetrachloroaurate) was added and heated to 95 °C. Then 5 mL of a 1% sodium citrate solution was added to the hot $HAuCl_4$ solution and heated almost to boiling. After the addition of sodium citrate blue staining appeared, which turned red within a few minutes. The whole process lasted 1-3 minutes. According to scanning electron microscopy, the diameter of the nanoparticles was $\sim$20 nm. Alternatively, we carried out the modification of the fabricated Ru structures by Au structures deposited from DMF solution of 3 mM $[(C_6H_5)_3P]AuCl$ (chloro(triphenylphosphine)gold(I)) upon the 532-nm irradiation at the laser power density and at the scanning speed used for the deposition of Ru.

Elemental and phase analysis

The morphology of the Ru-Au electrode material was investigated using scanning electron microscope Zeiss Supra 40 VP (Oberkochen, Germany). The elemental analysis of this material was accomplished using the energy dispersive X-ray (EDX) analyzer (INCA X-Act, Oxford Instruments, UK). The X-ray diffraction (XRD) analysis of the Ru-Au structures was performed using Bruker D2 Phaser diffractometer equipped with LynxEye detector (Karlsruhe, Germany). The X-ray photoelectron spectroscopy (XPS) data were obtained using a spectrometer Escalab 250Xi (Thermo Fisher Scientific, East Grinstead, UK).

Electrochemical studies

The cyclic voltammetry (CV) and differential pulse voltammetry (DPV) were applied for investigation of the electrochemical properties of the Ru-Au electrode material. This electrode was used as the working electrode in a standard three-electrode electrochemical cell that includes Ag/AgCl electrode and Pt wire as reference and counter electrodes, respectively. The voltammetric data were recorded in phosphate-buffered saline background solution (0.1 M PBS, pH 7.0) at room temperature using Corrtest CS300 potentiostat

(Woham Corrtest Instruments Ltd., China). Cyclic voltammetric measurements were performed vs. Ag/AgCl at a scan rate of 50 mV s^{-1} between -0.4 and 0.7 V. The selectivity of the fabricated electrode toward EP was investigated using DPV method in a mixture of EP solutions with different concentrations of dopamine (DA) and ascorbic acid (AA) as interfering analytes.

Results and discussion

We fabricated Ru-based microstructures (electrodes), including bare Ru, Ru-Au and Ru-AuNPs, on the surface of glass using the methodology described in the "Materials and Methods" section. The morphologies of these electrodes were examined using scanning electron microscopy (SEM) (Figs. 1a-f). According to micrographs shown in Fig. 1a, bare Ru electrode has a porous and well-developed non-planar surface. This result is consistent with those obtained in our recent studies on LCLD syntheses of similar electrode materials [42, 43]. Figs. 1b,c demonstrate SEM images of the Ru-Au electrode fabricated using consecutive deposition of Au on the surface of bare Ru upon the 532-nm laser irradiation. This composite material also has a highly developed surface consisting of large NPs, which are covered with particles of smaller diameter (20-80 nm). At smaller magnification we observe larger particles and cracks several microns in size on the surface of the Au-Ru electrode (Fig. 1b, inset). Figs. 1e,f show SEM images of Ru-AuNPs electrode produced by laser-induced modification of the surface of bare Ru with Au particles deposited from the colloidal solution containing AuNPs (Fig. 1d). The surface of Ru electrode modified with Au particles exhibits a hierarchical nature consisting of spherical NPs of small diameter (about 10 nm) and cracks with a width of about 0.5 μm that are also filled with NPs of the same or even smaller diameter. It is clear that such structural organization of Ru with AuNPs increases the active surface of bare Ru electrode material to a greater extent compared to results of successive laser-assisted deposition of Ru and Au, which makes Ru-AuNPs electrode the most attractive for our further studies.

The EDX studies (Fig. 2a) revealed that the Ru-AuNPs electrode is mainly composed of Ru (65 wt.%) and Au (22 wt.%). The presence of other elements in the EDX spectra, such as carbon, oxygen, magnesium, sodium, potassium and chlorine, can be related to the substrate material, i.e. glass. The EDX data is supported by the results of the XRD analysis (Fig. 2b). As one can see, the recorded XRD patterns of Ru-AuNPs can be attributed to the corresponding metallic phases, i.e. Ru and Au, as well as the oxide phase attributed to RuO_2. The surface of Ru-AuNPs electrode was also investigated using XPS technique (Figs. 2c,d). The presence of Au^0 is confirmed by the presence of two asymmetric XPS signals at ~84.0 eV and ~87.8 eV in the Au4f region [45] as shown in Fig. 2c. The XPS signal demonstrated in Fig. 2d has two peaks centered at ~280.2 and ~284.3 eV, which can be associated with metallic Ru^0 [46].

To evaluate the electrode with the largest electroactive surface area, corresponding cyclic voltammograms (CVs) were recorded in 0.1 M PBS (pH 7.0) in absence of any analyte. Besides the Ru, Ru-Au, and Ru-AuNPs electrodes, Au and Au-Ru electrodes were considered. Au and Au-Ru electrodes were obtained and characterized in our previous study [24]. The obtained CVs are shown in Fig. 4a. According to Fig. 4a, the largest CV area is observed for the Ru-based electrode modified by Au particles. Thus, the Ru-AuNPs electrode possesses the largest electroactive surface area, and can be considered as the best candidate for further voltammetric studies compared to other synthesized materials. This observation is also consistent with the results of SEM analysis shown in Figs. 1e,f.

The voltammetric measurements for different concentrations of EP in 0.1 M PBS were performed with the Ru-AuNPs electrode by scanning the potential from -0.4 V to

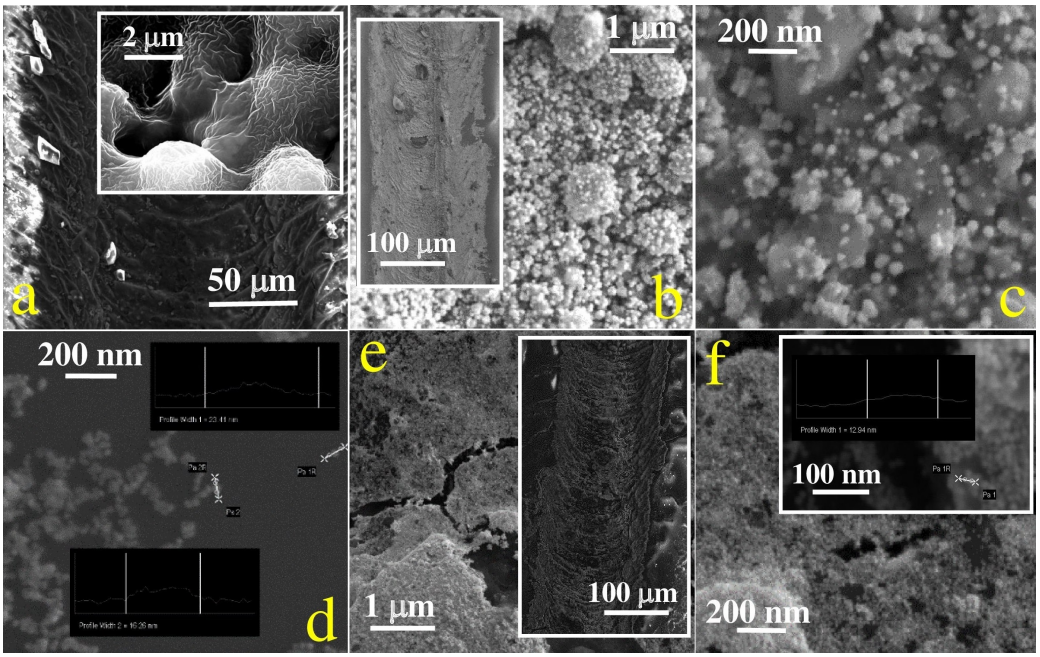

Figure 1. (a) SEM images of Ru microstructures (electrode) deposited on glass upon the 532-nm laser irradiation. (b,c) SEM images of Ru-Au electrode obtained using consecutive laser deposition of Au on the surface of the fabricated Ru microstructures. (d) SEM image of AuNPs containing in the colloidal solution prepared as described in [44]. (e,f) SEM images of Ru-AuNPs electrode obtained via modification of the surface of the fabricated Ru microstructures by Au particles deposited from the colloidal solution with AuNPs upon the 532-nm laser irradiation.

0.7 V at the scan rate of 50 mV s^{-1} (Fig. 4b). Six broad regions can be identified in the recorded cyclic voltammograms: the oxidation regions -0.27 – -0.06 V (**I**), -0.07 – 0.19 V (**II**), 0.2 – 0.62 V (**III**) and the reduction regions 0.64 – 0.32 V (**IV**), 0.31 – -0.12 V (**V**), -0.13 – -0.37 V (**VI**). In order to understand the processes that correspond to each of the redox regions, we referred to the mechanism of the electrochemical EP oxidation proposed earlier (Fig. 3, [1,47]). According to the proposed mechanism and the results of our previous studies [24,42], **I** and **II** can be attributed to the electrocatalytic EP oxidation process that involves the Ru^{2+}/Ru^{3+} redox reaction. On the other hand, **III** may involve such redox reactions as Ru^{0}/Ru^{3+} and Ru^{3+}/Ru^{4+} [18,42]. These electron transfer processes are accompanied by EP oxidation, i.e. oxidation of its two hydroxyl groups with the formation of epinephrinequinone. The region **III** can be considered as a very broad signal in which two separate peaks can be distinguished. The presence of two peaks centered at ∼0.25 V and ∼0.41 V can be explained by the fact that two hydroxyl groups of EP have different positions relative to other substituents in the benzene ring [24]. Additionally, a signal in the region of oxidation peak at 0.25 V can appear as a result of EP interaction with Au deposited on the surface of Ru electrode [19]. These observations can be a good evidence that an efficient catalysis of EP occurs on the surface of Ru modified with Au particles. We assume that other intermediates, leucoadrenochrome and adrenochrome, are formed at potentials higher than 0.6 V [1,24].

The regions **IV**, **V**, and **VI** were attributed to the reduction processes. The regions **IV** and **VI** are related to catalytic reduction of epinephrinequinone to EP on the surface of the metallic and oxide forms of Ru, respectively [48]. In turn, **V** can be assigned to reduction of epinephrinequinone to EP on the surface of Au [49]. The reversible reaction

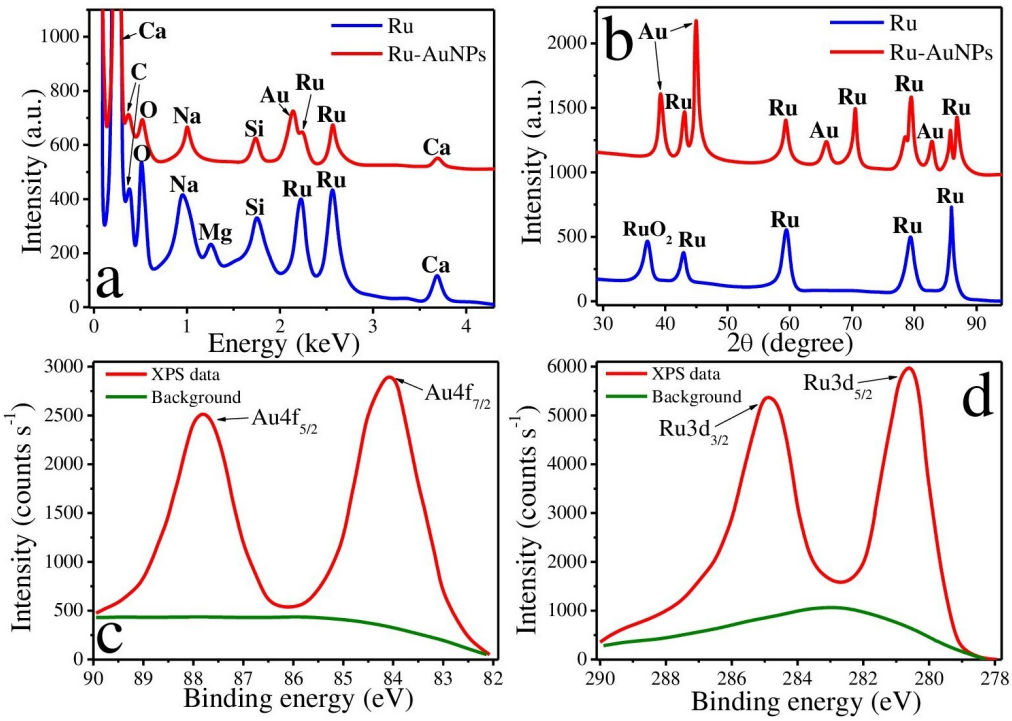

Figure 2. (a) EDX spectra and (b) XRD patterns of bare Ru and Ru-AuNPs electrodes. XPS spectra analysis of Ru-AuNPs electrode: (c) Au4f and (d) Ru3d regions.

between leucoadrenochrome and adrenochrome should occur at potentials lower than -0.3 V [1, 24].

Table 1. Comparison of various modified electrodes used for EP sensing.

Modified electrode	**Linear range (μM)**	**LOD (μM)**	**Reference**
Ru-AuNPs	0.01-5 and 5-500	0.0061 and 0.0178	This study
Au-MWCNT-PANI-RuO_2	4.9-76.9	0.18	[18]
AuNPs/PDA/AN	1- 1000	0.26	[23]
Au-Ru composite	0.01-10 and 10-1000	0.009 and 0.02	[24]
glassy carbon electrode (GCE) modified by AuNPs	0.05-1000	0.0017	[26]
Nanoporous spongelike Au-Ag films	25-700	5.05	[47]
Au-Pd core-shell nanocrystals	0.001-1000	0.0012	[50]
NiO-rGO hybrid composite	0.05-1000	0.01	[51]
ZrO2/ZnO nanocomposites	0.8-420	0.039	[52]
nanosized copper telluride (nps-CuTe)	5-60	0.018	[53]
nanoporous gold (h-nPG) microneedle	0-850	0.1	[54]
PPY/ZnO/AuNp/ RGO/GCE	0.6-500	0.06	[55]
CP-AuNPs nanocomposite	10-640	1.4	[56]

For quantitative determination of such hydrophobic compound as EP, which is contained in biological fluids in extremely low concentrations, we turned to differential pulse voltammetry (DPV) as one of the most sensitive electrochemical methods. The dependence of DPV current signal on EP concentration is shown in Fig. 4c. According to this figure, the increase of EP concentration leads to a gradual increase of DPV current accompanied by the shift of the peak from 0.26 V to 0.37 V. Fig. 4d shows the calibration curve derived as the dependence of signal intensity at 0.28 V on EP concentration. Two linear ranges are observed on this curve: 0.01-5 μM (R^2=0.998) and 5-500 μM (R^2=0.999). Measurements in the first linear range exhibit high sensitivity, i.e. we obtained a fast growth of DPV current upon increase of EP concentration. Measurements in the second linear range exhibit much lower sensitivity, which is typically related to

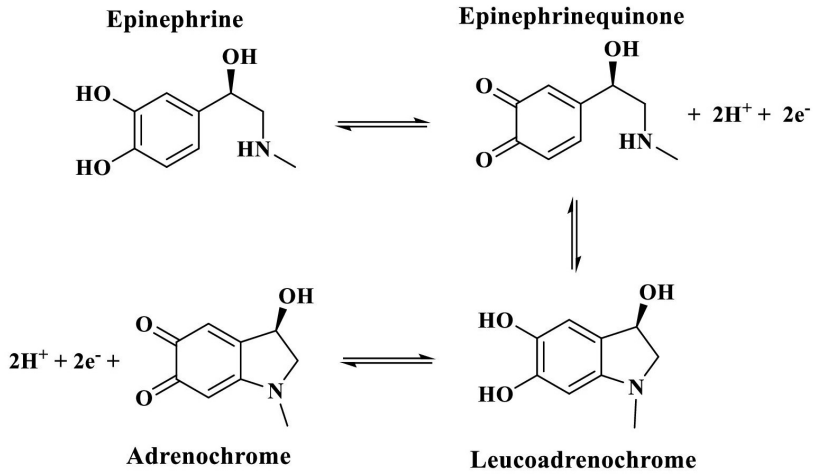

Figure 3. The mechanism of the electrochemical oxidation of EP [47].

the absorption of intermediates at high concentrations of an analyte [57]. The high sensitivity of measurements at low concentrations of EP can be attributed to the highly developed hierarchical structure of the Ru-AuNPs electrode surface. A significantly lower sensitivity of measurements at high EP concentrations may be associated with strong absorption of leucoadrenochrome and/or adrenochrome that are formed as intermediate species (see Fig. 3) during EP oxidation on the surface of the electrode [58].

The sensitivity values calculated for the first and second linear ranges are 46.9 and 2.1 μA μM^{-1} cm^{-2}, respectively. The detection limits (LOD = 3S/b, where S is the standard deviation from linearity, b is the sensitivity calculated as slope of the calibration curve) for these linear ranges were estimated to be 6.1 and 17.8 nM, respectively. A comparison of electrochemical characteristics of the Ru-AuNPs electrode proposed in this study with the same characteristics of similar modified electrodes used for EP sensing is presented in Tab. **??**. Ru-AuNPs sensor demonstrates the linear response range and detection limit that are comparable to those of the best EP sensors. In addition, Ru-AuNPs sensor reveals increased sensitivity (46.9 μA μM^{-1} cm^{-2} within the first linear range), while a typical value for sensitivity of detection of EP and many other hydrophobic metabolites is less than 10 μA μM^{-1} cm^{-2} [1].

We also employed DVP technique to examine the selectivity of EP detection in the presence of dopamine and ascorbic acid (Fig. 4e). These compounds were selected as interfering substances that commonly coexist with EP in biological fluids and can interfere with its voltammetric determination. DPV responses obtained from the mixture of 0.1 M PBS solution with EP, the 10-fold excess of dopamine, and the 10-fold excess of ascorbic acid exhibits no significant changes as compared to DVP responses obtained from 0.1 M PBS solution containing only EP. Therefore, the fabricated Ru-AuNPs sensor conserve a good selectivity for EP sensing in the presence of such physiologically important interfering substances as dopamine and ascorbic acid.

The repeatability of the Ru-AuNPs electrode was evaluated by performing five consecutive DVP measurements for 5 μM EP in 0.1 M PBS using the same electrode. The relative standard deviation (RSD) was estimated to be 0.45 %. The stability of Ru-AuNPs electrode was examined during 30 days, DPV response was recorded for 5 μM EP in 0.1 M PBS each ten days. It was observed that more than 98 % of the initial current response was retained after a month (Fig. 4f). The reproducibility of the electrochemical properties was tested with five different Ru-AuNPs electrodes. For this purpose, DPV measurements were performed for 5 μM EP in 0.1 M PBS. The calculated RSD was less than 2.50 %.

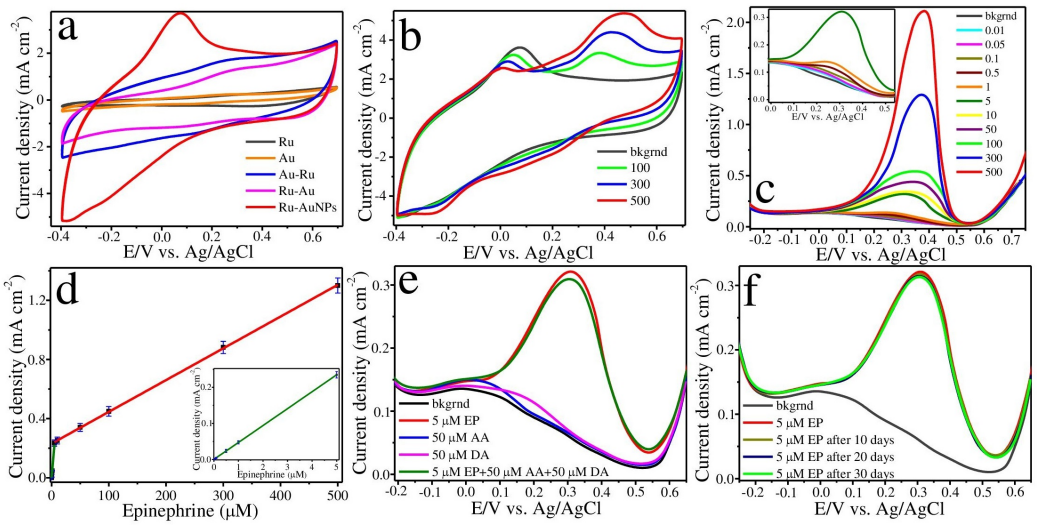

Figure 4. (a) CVs of Ru, Au, Au-Ru, Ru-Au and Ru-AuNPs electrodes recorded in 0.1 M PBS. (b) CVs of Ru-AuNPs recorded in 0.1 M PBS with different EP concentrations. (c) Effect of the EP concentration on the DPV current signals obtained using Ru-AuNPs electrode. (d) Corresponding calibration curves of the current density against EP concentration shown in μM. (e) DPV response of Ru-AuNPs in 0.1 M PBS (pH 7.0) containing pure 5 μM EP, pure 50 μM dopamine (DA), pure 50 μM ascorbic acid (AA) and their mixture. (f) The stability measurements of one fabricated Ru-AuNPs electrode carried out in 0.1 M PBS with 5 μM EP during 30 days.

Conclusions

In this study, we developed a technique for voltammetric non-enzymatic detection of epinephrine using the Ru-based electrode modified by Au particles. The electrode material was fabricated on the surface of a biologically inert dielectric substrate (glass) using the method of laser-induced metal deposition from solution. The addition of Au significantly increased the electrocatalytic activity of the Ru-based electrode in comparison with pure Ru. The fabricated electrode demonstrated good electrochemical performance appropriate for efficient voltammetric EP sensing. DPV studies showed that the Ru-Au sensor has two linear ranges of EP determination: 0.01-5 μM and 5-500 μM. The most promising electrochemical characteristics were found for the first linear range, which demonstrates the highest sensitivity (46.9 μA μM^{-1} cm^{-2}) and the lowest detection limit (6.1 nM). The sensitivity and the limit of detection for the second linear range were found to be 2.1 μA μM^{-1} cm^{-2} and 17.8 nM, respectively. Thus, the proposed approach opens up an opportunity of creating low-cost voltammetric sensor platforms for efficient detection of such hydrophobic metabolites as EP in a physiological environment.

Acknowledgments

This research is partially funded by the Ministry of Science and Higher Education of the Russian Federation as part of World-class Research Center program: Advanced Digital Technologies (contract No. 075-15-2022-311 dated by 20 April 2022). The research was partially funded by the Ministry of Health of the Russian Federation State task agreement No. 056-00012-23-01. The study was partially supported by the Ministry of Education and Science of the Russian Federation (Project FSRM-2023-0005).

The authors express their gratitude to the Research park of St. Petersburg State University "Interdisciplinary Resource Center for Nanotechnologies", "Center for Magnetic Resonance", "Center for Optical and Laser Research", "Center for X-ray Diffraction Studies", "Centre for Physical Methods of Surface Investigation", "Center for Chemical Analysis and Materials Research", "Center for Magnetic Resonance", "Center for Molecular and Cell Technologies". The authors also acknowledge computational resources of Peter the Great Saint-Petersburg Polytechnic University Supercomputing Center (www.spbstu.ru). The authors also acknowledge the Federal Joint Research Center "Material science and characterization in advanced technology" for providing SEM characterization.

References

1. Zahra Panahi, Luciana Custer, and Jeffrey Mark Halpern. Recent advances in non-enzymatic electrochemical detection of hydrophobic metabolites in biofluids. *Sens. Actuators Rep.*, 3:100051, 2021.

2. S Bonyadi, Kh Ghanbari, and M Ghiasi. All-electrochemical synthesis of a three-dimensional mesoporous polymeric gc 3 n 4/pani/cdo nanocomposite and its application as a novel sensor for the simultaneous determination of epinephrine, paracetamol, mefenamic acid, and ciprofloxacin. *New J. Chem.*, 44(8):3412–3424, 2020.

3. Wachira Wongtanasarasin, Karan Srisurapanont, and Daniel K Nishijima. How epinephrine administration interval impacts the outcomes of resuscitation during adult cardiac arrest: A systematic review and meta-analysis. *J. Clin. Med.*, 12(2):481, 2023.

4. Geneva D Mehta, Joumane El Zein, Isis Felippe Baroni, Myrha Qadir, Carol Mita, Rebecca E Cash, and Carlos A Camargo Jr. Epinephrine treatment of food-induced and other cause anaphylaxis in united states and canadian emergency departments: a systematic review and meta-analysis. *Expert Rev. Clin. Immunol.*, (just-accepted), 2023.

5. M Taei, H Hadadzadeh, F Hasanpour, N Tavakkoli, and M Hadadi Dolatabadi. Simultaneous electrochemical determination of ascorbic acid, epinephrine, and uric acid using a polymer film-modified electrode based on au nanoparticles/poly (3, 3',5,5'-tetrabromo-m-cresolsulfonphthalein). *Ionics*, 21:3267–3278, 2015.

6. Mohammad Mazloum-Ardakani, Hadi Beitollahi, Mohammad Kazem Amini, Bibi-Fatemeh Mirjalili, and Fakhradin Mirkhalaf. Simultaneous determination of epinephrine and uric acid at a gold electrode modified by a 2-(2, 3-dihydroxy phenyl)-1, 3-dithiane self-assembled monolayer. *J. Electroanal. Chem.*, 651(2):243–249, 2011.

7. Ewa Wierzbicka, Małgorzata Szultka-Młyńska, Bogusław Buszewski, and Grzegorz D Sulka. Epinephrine sensing at nanostructured au electrode and determination its oxidative metabolism. *Sens. Actuators B Chem.*, 237:206–215, 2016.

8. Hadi Beitollahi, Mohadeseh Safaei, and Somayeh Tajik. Voltammetric and amperometric sensors for determination of epinephrine: A short review (2013-2017). *J. Electrochem. Sci. Eng.*, 9(1):27–43, 2019.

9. Eric Bakker and Martin Telting-Diaz. Electrochemical sensors. *Anal. Chem.*, 74(12):2781–2800, 2002.

10. Mohamed H Hassan, Cian Vyas, Bruce Grieve, and Paulo Bartolo. Recent advances in enzymatic and non-enzymatic electrochemical glucose sensing. *Sensors*, 21(14):4672, 2021.

11. Muhammad Faiz Md Shakhih, Anis Suzziani Rosslan, Anas Mohd Noor, Santheraleka Ramanathan, Azwan Mat Lazim, and Asnida Abdul Wahab. Enzymatic and non-enzymatic electrochemical sensor for lactate detection in human biofluids. *J. Electrochem. Soc.*, 168(6):067502, 2021.

12. Dae-Woong Hwang, Saram Lee, Minjee Seo, and Taek Dong Chung. Recent advances in electrochemical non-enzymatic glucose sensors–a review. *Anal. Chim. Acta*, 1033:1–34, 2018.

13. Sejin Park, Hankil Boo, and Taek Dong Chung. Electrochemical non-enzymatic glucose sensors. *Anal. Chim. Acta*, 556(1):46–57, 2006.

14. Jajack Heikenfeld, Andrew Jajack, Jim Rogers, Philipp Gutruf, Lei Tian, Tingrui Pan, Ruya Li, Michelle Khine, Jintae Kim, and Juanhong Wang. Wearable sensors: modalities, challenges, and prospects. *Lab on a Chip*, 18(2):217–248, 2018.

15. Pitchaimani Veerakumar, Shih-Tung Hung, Pei-Qi Hung, and King-Chuen Lin. Review of the design of ruthenium-based nanomaterials and their sensing applications in electrochemistry. *J. Agric. Food Chem.*, 70(28):8523–8550, 2022.

16. P Muthukumaran, C Sumathi, J Wilson, and G Ravi. Enzymeless biosensor based on β-nis@ rgo/au nanocomposites for simultaneous detection of ascorbic acid, epinephrine and uric acid. *RSC Adv.*, 6(99):96467–96478, 2016.

17. Danyu He, Pu Zhang, Shehong Li, and Hongxia Luo. A novel free-standing cvd graphene platform electrode modified with aupt hybrid nanoparticles and l-cysteine for the selective determination of epinephrine. *J. Electroanal. Chem.*, 823:678–687, 2018.

18. Tebogo P Tsele, Abolanle S Adekunle, Omolola E Fayemi, and Eno E Ebenso. Electrochemical detection of epinephrine using polyaniline nanocomposite films doped with tio2 and ruo2 nanoparticles on multi-walled carbon nanotube. *Electrochim. Acta*, 243:331–348, 2017.

19. Dina M Fouad, Waleed A El-Said, et al. Selective electrochemical detection of epinephrine using gold nanoporous film. *J. Nanomater.*, 2016, 2016.

20. Adam Gorczyński, Maciej Kubicki, Klaudia Szymkowiak, Teresa Łuczak, and Violetta Patroniak. Utilization of a new gold/schiff-base iron (iii) complex composite as a highly sensitive voltammetric sensor for determination of epinephrine in the presence of ascorbic acid. *RSC Adv.*, 6(104):101888–101899, 2016.

21. Shreanshi Agrahari, Ankit Kumar Singh, Ravindra Kumar Gautam, and Ida Tiwari. Voltammetric analysis of epinephrine using glassy carbon electrode modified with nanocomposite prepared from co-nd bimetallic nanoparticles, alumina nanoparticles and functionalized multiwalled carbon nanotubes. *Environ. Sci. Pollut. Res.*, pages 1–18, 2022.

22. Majid Arvand, Zahra Khoshkholgh, and Shiva Hemmati. Trace level detection of guanine and adenine and evaluation of damage to dna using electro-synthesised zns@ cds core-shell quantum dots decorated graphene oxide nanocomposite. *J. Electroanal. Chem.*, 817:149–159, 2018.

23. Shanshan Zhan, Caihong Xu, Jiandan Chen, Qi Xiao, Zhenzeng Zhou, Zhiyuan Xing, Chunchuan Gu, Zhengzhi Yin, and Hongying Liu. A novel epinephrine biosensor based on gold nanoparticles coordinated polydopamine-functionalized acupuncture needle microelectrode. *Electrochim. Acta*, 437:141468, 2023.

24. Maxim S Panov, Alexey P Zakharov, Evgenia M Khairullina, Ilya I Tumkin, Andrey S Mereshchenko, Dmitrii M Nikolaev, Andrey V Vasin, and Mikhail N Ryazantsev. Au–ru composite for enzyme-free epinephrine sensing. *Chemosensors*, 10(12):513, 2022.

25. Peng Lei, Ying Zhou, Ruiqi Zhu, Chuan Dong, Si Wu, and Shaomin Shuang. Facilely synthesized ultrathin ni6mno8@ c nanosheets: excellent electrochemical performance and enhanced electrocatalytic epinephrine sensing. *Sens. Actuators B Chem.*, 326:128863, 2021.

26. Dimpo S Sipuka, Tsholofelo I Sebokolodi, Foluke OG Olorundare, Charles Muzenda, Oluchi V Nkwachukwu, Duduzile Nkosi, and Omotayo A Arotiba. Electrochemical sensing of epinephrine on a carbon nanofibers and gold nanoparticle-modified electrode. *Electrocatalysis*, 14(1):9–17, 2023.

27. Sascha Engelhardt. Direct laser writing. In *Laser Technology in Biomimetics: Basics and Applications*, pages 13–65. Springer, 2014.

28. Jan-Otto Carlsson and Peter M Martin. Chemical vapor deposition. In *Handbook of Deposition Technologies for films and coatings*, pages 314–363. Elsevier, 2010.

29. Gerard Cummins and Marc PY Desmulliez. Inkjet printing of conductive materials: a review. *Circuit World*, 38(4):193–213, 2012.

30. John C Miller. *Laser ablation: principles and applications*, volume 28. Springer Science & Business Media, 2013.

31. Mizue Mizoshiri, Kenta Nishitani, and Seiichi Hata. Effect of heat accumulation on femtosecond laser reductive sintering of mixed cuo/nio nanoparticles. *Micromachines*, 9(6):264, 2018.

32. Yung-Lang Yang, Chin-Chi Hsu, Tien-Li Chang, Long-Sheng Kuo, and Ping-Hei Chen. Study on wetting properties of periodical nanopatterns by a combinative technique of photolithography and laser interference lithography. *Appl. Surf. Sci.*, 256(11):3683–3687, 2010.

33. Jyotsna Dutta Majumdar and Indranil Manna. *Laser-assisted fabrication of materials*, volume 161. Springer Science & Business Media, 2012.

34. Vladimir Alekseevich Kochemirovsky, M Yu Skripkin, Yu S Tveryanovich, Andrey S Mereshchenko, Artem Olegovich Gorbunov, Maksim Sergeevich Panov, Il'ya Igorevich Tumkin, and Sergei Vladimirovich Safonov. Laser-induced copper deposition from aqueous and aqueous–organic solutions: State of the art and prospects of research. *Russ. Chem. Rev.*, 84(10):1059, 2015.

35. Jianming Zhang, Mohamed Chaker, and Dongling Ma. Pulsed laser ablation based synthesis of colloidal metal nanoparticles for catalytic applications. *J. Colloid Interface Sci.*, 489:138–149, 2017.

36. Arseniy I Kuznetsov, Andrey B Evlyukhin, Manuel R Gonçalves, Carsten Reinhardt, Anastasia Koroleva, Maria Luisa Arnedillo, Roman Kiyan, Othmar Marti, and Boris N Chichkov. Laser fabrication of large-scale nanoparticle arrays for sensing applications. *ACS Nano*, 5(6):4843–4849, 2011.

37. C Shao, Y Zhao, N Chen, H Zhu, L Wang, H Sun, and L Qu. Application of laser micro-nano-fabrication in sensing field. *Zhongguo Jiguang/Chin. J. Lasers.*, 2021.

38. Patrick Z El-Khoury, Alexander N Tarnovsky, Igor Schapiro, Mikhail N Ryazantsev, and Massimo Olivucci. Structure of the photochemical reaction path populated via promotion of cf2i2 into its first excited state. *J. Phys. Chem. A*, 113(40):10767–10771, 2009.

39. Evgeniia Khairullina, Andrey Shishov, Dmitry Gordeychuk, Lev Logunov, Aleksandra Levshakova, Vladimir B Sosnovsky, Aleksandra Koroleva, Vladimir Mikhailovsky, Evgeny L Gurevich, Ivan Chernyshov, et al. Rapid and effective method of laser metallization of dielectric materials using deep eutectic solvents with copper acetate. *J. Mater. Sci.*, pages 1–15, 2023.

40. Evgeniia M Khairullina, Ilya I Tumkin, Daniil D Stupin, Alexandra V Smikhovskaia, Andrey S Mereshchenko, Alexey I Lihachev, Andrey V Vasin, Mikhail N Ryazantsev, and Maxim S Panov. Laser-assisted surface modification of ni microstructures with au and pt toward cell biocompatibility and high enzyme-free glucose sensing. *ACS Omega*, 6(28):18099–18109, 2021.

41. Maxim S. Panov, Evgeniia M. Khairullina, Filipp S. Vshivtcev, Mikhail N. Ryazantsev, and Ilya I. Tumkin. Laser-induced synthesis of composite materials based on iridium, gold and platinum for non-enzymatic glucose sensing. *Materials*, 13(15):3359, 2020.

42. Maxim S Panov, Anastasiia E Grishankina, Daniil D Stupin, Alexey I Lihachev, Vladimir N Mironov, Daniil M Strashkov, Evgeniia M Khairullina, Ilya I Tumkin, and Mikhail N Ryazantsev. In situ laser-induced fabrication of a ruthenium-based microelectrode for non-enzymatic dopamine sensing. *Materials*, 13(23):5385, 2020.

43. Daniil D Stupin, Anna A Abelit, Andrey S Mereshchenko, Maxim S Panov, and Mikhail N Ryazantsev. Copper–ruthenium composite as perspective material for bioelectrodes: Laser-assisted synthesis, biocompatibility study, and an impedance-based cellular biosensor as proof of concept. *Biosensors*, 12(7):527, 2022.

44. Lev A Dykman and Nikolay G Khlebtsov. Methods for chemical synthesis of colloidal gold. *Russ. Chem. Rev.*, 88(3):229, 2019.

45. MP Casaletto, A Longo, A Martorana, A Prestianni, and AM Venezia. Xps study of supported gold catalysts: the role of au0 and au+ δ species as active sites. *Surf. Interface Anal.*, 38(4):215–218, 2006.

46. David J Morgan. Resolving ruthenium: Xps studies of common ruthenium materials. *Surf. Interface Anal.*, 47(11):1072–1079, 2015.

47. Ewa Wierzbicka and Grzegorz D Sulka. Nanoporous spongelike au–ag films for electrochemical epinephrine sensing. *J. Electroanal. Chem.*, 762:43–50, 2016.

48. Liang Wang, Junyue Bai, Pengfei Huang, Hongjing Wang, Liying Zhang, and Yuqing Zhao. Electrochemical behavior and determination of epinephrine at a penicillamine self-assembled gold electrode. *Int. J. Electrochem. Sci.*, 1(3):238–249, 2006.

49. Toktam Tavana, Mohammad A Khalilzadeh, Hassan Karimi-Maleh, Ali A Ensafi, Hadi Beitollahi, and Daryoush Zareyee. Sensitive voltammetric determination of epinephrine in the presence of acetaminophen at a novel ionic liquid modified carbon nanotubes paste electrode. *J. Mol. Liq.*, 168:69–74, 2012.

50. Wenhao Dong, Yipeng Ren, Zhixue Bai, Jun Jiao, Yuan Chen, Bingkai Han, and Qiang Chen. Synthesis of tetrahexahedral au-pd core–shell nanocrystals and reduction of graphene oxide for the electrochemical detection of epinephrine. *J. Colloid Interface Sci.*, 512:812–818, 2018.

51. AG Ramu, Ahmad Umar, Ahmed A Ibrahim, Hassan Algadi, Yousif SA Ibrahim, Yao Wang, Marlia M Hanafiah, P Shanmugam, and Dongjin Choi. Synthesis of porous 2d layered nickel oxide-reduced graphene oxide (nio-rgo) hybrid composite for the efficient electrochemical detection of epinephrine in biological fluid. *Environ. Res.*, 200:111366, 2021.

52. Qiwen Wang, Haipei Si, Lihui Zhang, Ling Li, Xiaohong Wang, and Shengtian Wang. A fast and facile electrochemical method for the simultaneous detection of epinephrine, uric acid and folic acid based on zro2/zno nanocomposites as sensing material. *Anal. Chim. Acta*, 1104:69–77, 2020.

53. Susmita Pradhan, Mahuya Bhattacharyya Banerjee, Sudip Biswas, Nor Aliya Hamizi, Dipak K Das, Radhaballabh Bhar, Rajib Bandyopadhyay, and Panchanan Pramanik. An efficient simultaneous electrochemical detection of nanomolar epinephrine and uric acid using low temperature synthesized nano-sized copper telluride. *Electroanalysis*, 33(2):383–392, 2021.

54. Cristina Tortolini, Anthony EG Cass, Riccardo Pofi, Andrea Lenzi, and Riccarda Antiochia. Microneedle-based nanoporous gold electrochemical sensor for real-time catecholamine detection. *Mikrochim. Acta*, 189(5):180, 2022.

55. KH Ghanbari and A Hajian. Electrochemical characterization of au/zno/ppy/rgo nanocomposite and its application for simultaneous determination of ascorbic acid, epinephrine, and uric acid. *J. Electroanal. Chem.*, 801:466–479, 2017.

56. Sorina Alexandra Leau, Cecilia Lete, Cristian Matei, and Stelian Lupu. Electrochemical sensing platform based on metal nanoparticles for epinephrine and serotonin. *Biosensors*, 13(8):781, 2023.

57. Md Nurul Karim, Ji Eun Lee, and Hye Jin Lee. Amperometric detection of catechol using tyrosinase modified electrodes enhanced by the layer-by-layer assembly of gold nanocubes and polyelectrolytes. *Biosens. Bioelectron.*, 61:147–151, 2014.

58. Di Zhu, Huiyuan Ma, Qingfang Zhen, Jianjiao Xin, Lichao Tan, Chunjing Zhang, Xinming Wang, and Boxin Xiao. Hierarchical flower-like zinc oxide nanosheets in-situ growth on three-dimensional ferrocene-functionalized graphene framework for sensitive determination of epinephrine and its oxidation derivative. *Appl. Surf. Sci.*, 526:146721, 2020.